# Linear dichroism of acrylodan-labeled tropomyosin and myosin subfragment 1 bound to actin in myofibrils

Danuta Szczesna and Sherwin S. Lehrer
Department of Muscle Research, Boston Biomedical Research Institute, Boston, Massachusetts 02114; and Department of Neurology, Harvard Medical School, Boston, Massachusetts 02115

ABSTRACT Muscle contraction can be activated by the binding of myosin heads to the thin filament, which appears to result in thin filament structural changes. In vitro studies of reconstituted muscle thin filaments have shown changes in tropomyosin–actin geometry associated with the binding of myosin subfragment 1 to actin. Further information about these structural changes was obtained with fluorescence-detected linear dichroism of tropomyosin, which was labeled at Cys 190 with acrylodan and incorporated into oriented ghost myofibrils. The fluorescence from three sarcomeres of the fibril was collected with the high numerical aperture objective of a microscope and the dichroic ratio, $R(0/90°)$, for excitation parallel/perpendicular to the fibril, was obtained, which gave the average probe dipole polar angle, $\Theta$. For both acrylodan-labeled tropomyosin bound to actin in fibrils and in $Mg^{2+}$ paracrystals, $\Theta \simeq 52° \pm 1.0°$, allowing for a small degree of orientational disorder. Binding of myosin subfragment 1 to actin in fibrils did not change $\Theta$; i.e., the orientation of the rigidly bound probe on tropomyosin did not change relative to the actin axis. These data indicate that myosin subfragment 1 binding to actin does not appreciably perturb the structure of tropomyosin near the probe and suggest that the geometry changes are such as to maintain the parallel orientation of the tropomyosin and actin axes, a finding consistent with models of muscle regulation. Data are also presented for effects of MgADP on the orientation of labeled myosin subfragment 1 bound to actin in myofibrils.

## INTRODUCTION

Structural studies have suggested that $Ca^{2+}$ activation of muscle contraction causes a 10–15 Å movement of tropomyosin (Tm) on actin, which forms the basis of the steric blocking theory of thin filament muscle regulation (Huxley, 1972; Haselgrove, 1972; Parry and Squire, 1973). Evidence for such a large $Ca^{2+}$-induced Tm movement, however, has not as yet been found with the use of in vitro fluorescence energy transfer methods on reconstituted thin filaments (Tao et al., 1983; Miki, 1990). It has been known for sometime that the binding of myosin heads or subfragment 1 (S1) to actin can activate the thin filament both in solution (Bremel and Weber, 1972; Nagashima and Asakura, 1982; Lehrer and Morris, 1982; Williams et al., 1988) and in fibers (Goldman et al., 1984; Guth and Potter, 1987; Gordon et al., 1988; Millar and Homsher, 1990) so that $Ca^{2+}$ may modulate the activation by myosin head binding leading to the Tm–actin structural change. Indeed, the cooperative binding of S1 to actin in reconstituted thin filaments changes various fluorescence properties of labeled Tm (Ishii and Lehrer, 1985; Lehrer and Ishii, 1988; Szczęsna et al., 1989) with little effect of $Ca^{2+}$ in the absence of S1 (Ishii and Lehrer, 1987, 1990). In particular, changes in geometry between Tm and actin produced by cooperative S1 binding have been shown by fluorescence energy transfer between tryptophans on actin and acrylodan (AC) on Tm (Lehrer and Ishii, 1988).

To obtain further evidence for S1-induced changes in tropomyosin–actin interaction, fluorescence-detected linear dichroism (FDLD) studies on AC-labeled Tm incorporated into ghost myofibrils (myosin and Tm-troponin removed) are reported here. Myofibrils attached to a glass coverslip are particularly well suited for the measurement because of the high degree of order imposed by the organized filaments whereby the axes of Tm and actin helices are arranged parallel to the fibril axis. In this helical array, the cylindrically symmetrical orientation of the probe absorption dipole relative to the fibril axis gives the dichroism. FDLD data of ACTm bound to actin showed little or no change in dichroism on binding S1 to the I-bands. This suggests that the S1-induced geometry change of Tm takes place by maintaining the angle between the probe dipole and fiber axis. As controls for the dichroism experiments, effects of the binding of ADP to S1 on the dichroism of rhodamine-labeled S1 (IATR-S1) bound to ghost fibrils previously studied (Borejdo et al., 1982; Burghardt et al., 1983) are verified. New data on the dichroism of ACS1 bound to ghost fibrils are also reported.

Address correspondence to Department of Muscle Research, Boston Biomedical Research Institute, 20 Staniford St., Boston, MA 02114.
Dr. Szczesna's permanent address is Nencki Institute of Experimental Biology, 3 Pasteur Street, 02-093 Warsaw, Poland.

## EXPERIMENTAL

### Preparations

Muscle fibers were prepared from rabbit psoas muscle dissected into small bundles, tied to wooden sticks and stored at −15°C in 50:50 glycerol/buffer (10 mM sodium phosphate, pH 7.0) for several months. Myofibrils were prepared from a bundle of fibers by a short treatment with a polytron homogenizer, rid of membrane components by low speed centrifugation, and washed and stored in rigor buffer (0.03 M NaCl, 3 mM $MgCl_2$, 0.5 mM dithiothreitol (DTT), and 10 mM Hepes, pH 7.2). To prevent damage to the Z-lines by endogenous proteases, 0.5 mM phenylmethyl-sulfonyl fluoride was added.

Tm and myosin were purified from frog (*Rana temporaria*) and rabbit skeletal muscle, respectively. ααTm, purified as described earlier (Hvidt, 1986), was used because it contains one Cys per chain, allowing a specific labeling site. Rabbit skeletal myosin S1 was prepared by chymotryptic cleavage of myosin (Weeds and Pope, 1977) using $Mg^{2+}$ to selectively precipitate rod and undigested myosin (Okamoto and Sekine, 1985).

Labeling of ααTm with AC (6-Acryloyl-2-dimethylaminonaphthalene) was performed in a solution containing ~1 mg/ml protein in 4 M guanidine hydrochloride, 10 mM Hepes buffer, pH 7.5, and 1 mM EDTA for 3.5–4 h at room temperature with 5× molar excess of AC, conditions that have been shown to specifically label Cys 190 (Lehrer and Ishii, 1988). The reaction was quenched with 5 mM DTT and the solution was dialyzed to renature and remove unreacted reagents. The resulting molar labeling ratio of AC/Tm was 1.6, determined using $\epsilon_{365}$(AC) = 12,900 $M^{-1}$ $cm^{-1}$. Singly labeled Tm (sACTm) with [AC]/[Tm] = 0.22 was prepared by mixing the highly labeled Tm ([AC]/[Tm] = 1.6) with unlabeled Tm at a ratio of 1 to 5, respectively, in the presence of 5 M guanidine hydrochloride and 5 mM DTT, followed by dialysis to refold versus solution containing 0.5 M NaCl, 1 mM EDTA, 10 mM Hepes buffer, pH 7.5, and 0.1 mM DTT (Ishii and Lehrer, 1991). Myosin S1 was labeled either with AC or iodoacetyltetramethylrhodamine (IATR) by incubation of ~2 mg/ml of S1 for 14 h in the dark at 0°C with equimolar dye, conditions that have been shown to specifically label Cys 707 (SH1) (Borejdo et al., 1979). The solutions were quenched with 5 mM DTT and dialyzed versus rigor buffer. The resulting molar ratio of label to S1 was 0.3 and 1.0 for IATR and AC, respectively.

$Mg^{2+}$ paracrystals of Tm were obtained by dialyzing ACTm (~2 mg/ml) against buffer containing 25 $MgCl_2$, 25 mM Tris/HCl (pH 8.0), and 1 mM DTT at 5°C (Yagi, 1988).

### Methods

Glass coverslip spacers (0.13–0.17 mm) were used to construct 50 μl volume cells with detachable coverslip covers and openings on opposite sides. Fluorescence measurements were performed on fibrils that naturally attach to the coverslip when a drop of a fibril suspension is introduced onto the open cell and covered with another glass coverslip. A thin layer of silicone grease on the spacers held the cover on. Irrigation of the attached fibrils with various solutions was accomplished by placing a drop of solution at one edge and drawing off an equivalent volume of solution from the other edge with a piece of filter paper. Ghost myofibrils with intact actin-containing I-filaments were prepared by irrigation of the attached fibrils, first with modified Hasselbach–Schneider solution (0.5 M NaCl, 1 mM $MgCl_2$, 10 mM NaPPi, 20 mM phosphate buffer, pH 6.4). The Hasselbach–Schneider solution removes myosin-containing thick filaments, tropomyosin, and troponin from the thin filament (Yanagida and Oosawa, 1978) and only actin filaments remain attached to Z-discs (see Fig. 3, *a* and *b*). Solutions of ACTm, ACS1, or IATR-S1 (~1 mg/ml) were introduced followed by an albumin solution (0.5 mg/ml in rigor buffer) to decrease nonspecific adhesion of added labeled protein then rinsed with rigor buffer. A solution containing 0.3% D-glucose, glucose oxidase (0.16 mg/ml), and catalase (0.016 mg/ml) in rigor buffer was introduced into the cell to reduce oxygen (Englander et al., 1987). Before measurements, both open edges of the cells were closed with rubber cement to inhibit the penetration of oxygen from the atmosphere. This procedure minimized photobleaching. Solutions containing MgADP (5 mM) also contained 100 μg/ml of hexokinase to remove contaminating ATP (Borejdo et al., 1982).

### Measurements

Steady-state fluorescence spectra were obtained with a Spex Fluorolog 2/2/2 photon-counting fluorometer (Spex Industries, Inc., Edison, NJ) in the ratio mode with 4.5-nm and 9-nm band-pass for excitation and emission spectra, respectively. Polarization data were obtained on the Spex fluorometer (Spex Industries, Inc.) with Glan-Thompson prisms in the L format and corrected for grating artifacts as described earlier (Lehrer and Ishii, 1988).

For dichroism measurements, the cell containing the attached myofibrils was placed on a revolving stage of a fluorescence microscope (Axiovert, Carl Zeiss, Inc., Thornwood, NY). Light from a 50-W mercury lamp was linearly polarized with a Zeiss rotating film polarizer and directed onto the sample through a Zeiss dichroic mirror assembly (No. 14 for IATR and No. 05 for AC) and a 100×/1.3 NA Plan-Neofluar objective. An iris in the exciting light path selected two to three sarcomeres of the fibril. The emitted light from the illuminated sarcomeres was collected over a large solid angle by the objective and measured by photon counting using a Hamamatsu R928 PM (Hamamatsu Corp., Bridgewater, NJ) and a DM 3000 Spex Computer (Spex Industries, Inc.). Stray light was minimized with a pinhole aperture in the emission path, which overlapped the area selected by the iris. Measurements were taken with a Spex photon counting assembly (Spex Industries, Inc.) for excitation parallel and perpendicular to the fibril by recording the fluorescence for 30 s and averaging. Measurements were done for fibrils oriented parallel and perpendicular to the axis of the microscope to take into account instrumental effects. Each measurement was corrected for background fluorescence by recording the fluorescence from an area adjacent to the fibril. The background fluorescence was usually <15% of the fluorescence recorded from the selected area of the fibril. Data were also corrected for the inherent dichroism of the instrument by measuring fluorescence from a drop of solution of ACS1 and IATR-S1 on a coverslip parallel and perpendicular to the plane of the dichroic mirror. The ratio of the fluorescence collected in these two positions gave correction factors of 1.03 and 1.08 for the AC- and IATR-probe, respectively.

Photographs were made using Kodak T-MAX 3200 or ILFORD XP1 400 films with a Nikon camera (Nikon Inc., Melville, NY) attached to the microscope with short exposure times for phase-contrast (1/30–1/60 s) and long times (15–50 s) for fluorescence with a 100×/1.25 NA Achrostigmat objective.

### Calculations

The measured fluorescence, $F$, can be expressed as (Borejdo et al., 1982):

$$F = \tfrac{1}{2} \sin^2 \psi \sin^2 \Theta + \cos^2 \psi \cos^2 \Theta, \qquad (1)$$

where $\psi$ is the angle between the myofibillar axis and the polarization direction of the exciting light and $\Theta$ is the average polar angle between the absorption dipole of the dye and the fibril axis.

Rearranging Eq. 1:

$$F = K_1 + K_2 \cos^2 \psi, \tag{2}$$

where

$$K_1 = \tfrac{1}{2} \sin^2 \Theta \quad \text{and} \quad K_2 = (\cos^2 \Theta - \tfrac{1}{2} \sin^2 \Theta). \tag{3}$$

These equations assume that the high NA objective does not affect the polarization of the exciting light because the incident light is passed through a small diameter excitation field iris and because Köhler illumination is used, which results in parallel light at the specimen plane. The high NA of the collection optics insures that essentially all of the fluorescence is collected (Burghardt and Thompson, 1984).

The polar angle $\Theta$, in the absence of disorder, can be calculated from measurements of the dichroic ratio obtained from Eq. 1:

$$R = F(\psi = 0°)/F(\psi = 90°) = 2 \cot^2 \Theta. \tag{4}$$

To consider the effect of dipole disorder, the dichroic ratio $R'$ weighted by a Gaussian distribution for each fluorescence component was used in model calculations

$$R' = \frac{F'(0°)}{F'(90°)} = \frac{2 \int_0^{\pi} d\Theta \cos^2 \Theta \sin \Theta \exp\{-\tfrac{1}{2}[(\Theta - \Theta_0)/\sigma]^2\}}{\int_0^{\pi} d\Theta \sin^3 \Theta \exp\{-\tfrac{1}{2}[(\Theta - \Theta_0)/\sigma]^2\}}, \tag{5}$$

where $\Theta_0$ is the average angle of the dipole distribution and $\sigma$ is the width of the Gaussian curve. A computer program was used to calculate the effect of disorder given by the distribution width, $\sigma$, on $R'$ for different values of $\Theta_0$. The effects of increasing the width of the Gaussian distribution on $R'$ for various average polar angles, $\Theta_0$, are shown in Fig. 1. As can be seen, as the width increases toward isotropic values, $R' \rightarrow 1$, as expected.

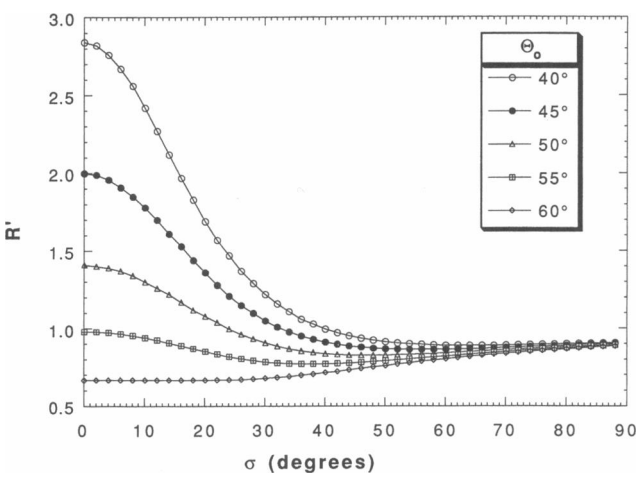


FIGURE 1 Family of theoretical curves relating measured dichroic ratio $R'(0°/90°)$ to the width of a Gaussian distribution, $\sigma$, of polar angle for different average angles, $\Theta_0$ (Eq. 5).

## RESULTS

### Characterization of labeled proteins

The solution polarization excitation spectra of IATR-S1 and ACS1 show a high degree of polarization in the wavelength region excited by the microscope dichroic filter assembly (Fig. 2). For IATR-S1, $P = 0.34$ at 546 nm, the Hg line isolated by the rhodamine band-pass excitation filter of the microscope. This value is in an excellent agreement with $P = 0.35$ measured previously for SH1-labeled S1 (Borejdo et al., 1982). For ACS1 the corrected emission and excitation peaks were at 490 and 388 nm, respectively, indicating a moderate degree of polarity (Weber and Farris, 1979; Prendergast et al., 1983) with $P = 0.43$ in the region of the two Hg lines isolated by the acrylodan band-pass filter (400–440 nm). For highly labeled ACTm the fluorescence excitation, emission, and polarization spectra were the same as for previously published rabbit skeletal Tm (Lehrer and Ishii, 1988) with $P = 0.35$ in the 420–440-nm region. The spectrum and polarization for sACTm in solution were similar to highly labeled ACTm with a slightly higher $P$ value in the 420–440 nm region ($P = 0.37$). As expected, $P \simeq 0 \pm 0.03$ for the free probes in solution. Thus, when AC is covalently bound to Cys 190 of Tm, it does not significantly rotate during its lifetime of 1.9 ns (Lehrer and Ishii, 1988) and can be considered to have a relatively fixed orientation for the dichroism experiments.

### Binding of labeled proteins to actin in myofibrils

On irrigation of the ghost myofibrils (Fig. 3 *b*) with labeled S1 or labeled Tm, an immediate increase in the density of the actin I-bands was observed with phase-contrast microscopy (Fig. 3, *c* and *e*). The increase was much greater for binding of S1 than for binding of Tm, most probably due to the higher resulting mass of S1 on the actin filament. There was an appearance of intense fluorescence in the actin bands associated with binding of labeled S1 or labeled Tm (Fig. 3, *d* and *f*). In both cases, the fluorescence was not associated with the Z-lines; this was not as obvious in the labeled S1 photograph (Fig. 3 *d*) as in the labeled Tm photograph (Fig. 3 *f*) because of overexposure.

### Dichroism of labeled S1 bound to ghost myofibrils

Studies with IATR-S1 were performed as a control in view of previous work with IATR-labeled fibers and

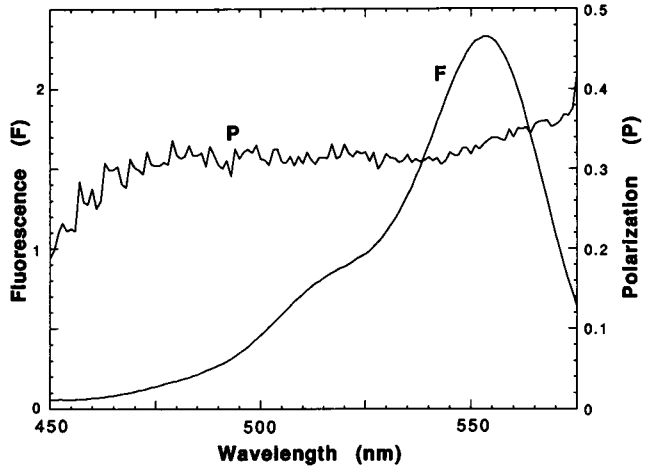


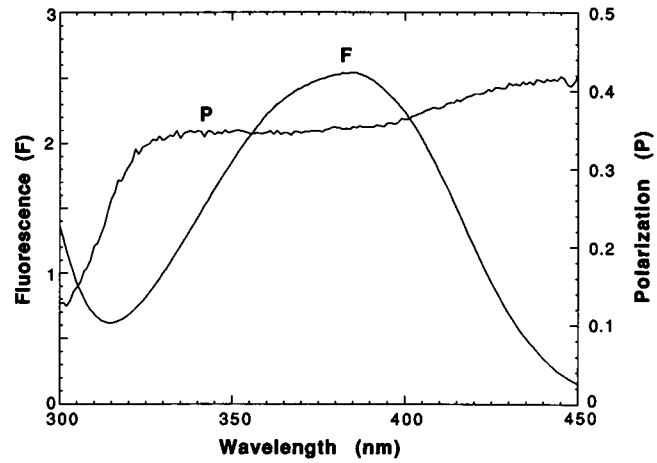


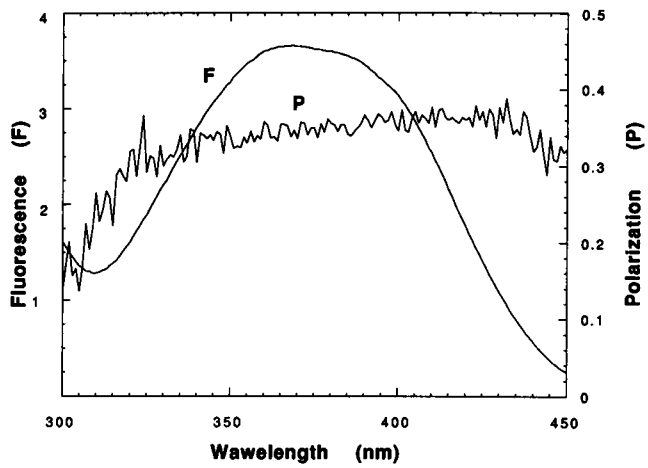


FIGURE 2 Fluorescence excitation ($F$) and polarization ($P$) spectra for (*a*) (*top left*) IATR-S1, (*b*) (*top right*) ACS1, and (*c*) (*bottom left*) sACTm determined in solution containing 0.03 M NaCl, 3 mM $MgCl_2$, and 10 mM Hepes buffer, pH 7.2 in 24°C. Emission wavelengths ($\lambda_{em}$) and protein concentrations were as follows: (*a*) $\lambda_{em}$ = 590 nm, [IATR-S1] = 4.7 μM; (*b*) $\lambda_{em}$ = 490 nm, [ACS1] = 0.8 μM; (*c*) $\lambda_{em}$ = 500 nm, [sACTm] = 20 μM.

fibrils, and ghost fibrils to which IATR-S1 had been bound (Borejdo et al., 1982; Burghardt et al., 1983). Our data show that in the absence of nucleotide, the dichroic angle $\Theta$ is ~60° which decreases to ~50° in the presence of ADP (Table 1). Although these values differ somewhat from the 69° and 47° of the previous results (Burghardt et al., 1983), there is a similar change from negative ($R < 1$; $\Theta > 54.74°$) to positive ($R > 1$; $\Theta < 54.74°$) dichroism due to the binding of ADP.

For ACS1 in the absence of nucleotide, the dichroism was also negative, with $\Theta \simeq 60°$ but, in contrast to the IATR label, binding of MgADP to S1 did not significantly change the orientation of the AC probe (Table 1). Thus, despite the similar probe dipole angle with respect to the fibril axis for AC and IATR on S1, different effects of S1 rotation were seen. This is probably due to different azimuthal angles with respect to S1 for the same polar angle probe locations, i.e., if S1 rotates about an axis parallel to the AC probe, no change would be observed. A lack of effect of ADP was also observed with 1,5-IAEDANS–modified S1 excited at 355 nm (Borejdo et al., 1982). However, an effect of ADP on the orientation of 1,5-IAEDANS–labeled S1 was observed for excitation at higher wavelengths where another transition with a different probe dipole is involved (Ajtai and Burghardt, 1987). The dependence of the fluorescence on the angle between the excitation polarization and the fibril axis for ACS1 bound to actin in myofibrils illustrates the agreement with Eq. 1 (Fig. 4). Similar data were obtained for IATR-S1.

## Dichroism of ACTm paracrystals and ACTm bound to ghost myofibrils

$Mg^{2+}$ paracrystals are needle-shaped tactoids of approximate dimensions 5–10 μm × 0.5–1 μm whose axis is coincident with the molecular axis of the Tm coiled-coil α-helix (Caspar et al., 1969). It was possible to obtain enough fluorescence intensity from single paracrystals to measure the dichroism (Table 1). The data show that the dichroism is slightly positive with $R = 1.15 \pm 0.06$, which corresponds to $\Theta \simeq 53°$ relative to the molecular axis. For ACTm incorporated into ghost myofibrils (Fig. 3, *e* and *f*) $R = 1.21 \pm 0.09$ and $R = 1.4 \pm 0.1$ for highly and

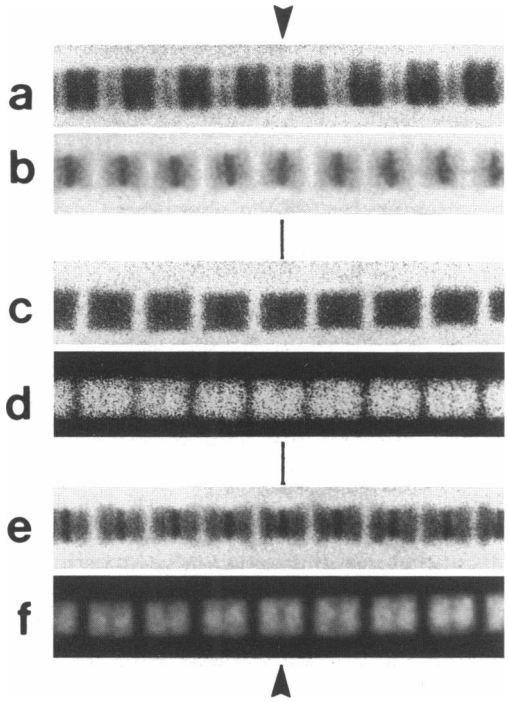


FIGURE 3 Pattern of binding of ACS1 and ACTm to ghost myofibrils. The myofibrils were photographed using phase-contrast (*a*, *b*, *c*, and *e*) with a 100×/1.25 NA Achrostigmat objective or epifluorescence illumination method (*d*, *f*) with a 100×/1.3 NA Plan-Neofluar objective. (*a*) Intact myofibril; (*b*) Ghost myofibril obtained by irrigating intact fibrils with Hasselbach-Schneider solution. Note loss of myosin-containing A-bands leaving actin-containing I-bands attached to Z-lines; (*c* and *d*) ACS1 bound to actin in ghost myofibrils; (*e* and *f*) ACTm incorporated into actin-containing I-filaments, showing increased I-band density in phase-contrast. The arrowheads mark the Z-line. The distance between adjacent Z-lines is 2.5–3 μm. All ghost myofibrils were finally rinsed with rigor buffer (for details see Methods).

singly labeled Tm, respectively (Table 1). On binding S1 to the ACTm-containing ghost fibrils, a further increase in density in phase contrast was observed in the I-bands, indicating that the S1 did indeed bind to the actin as expected and as seen with the labeled S1 studies reported above. This binding of S1 did not affect the ACTm probe angle (for both highly and singly labeled Tm) within experimental error, whether or not ADP was present (Table 1). The measured angle $\Theta = 52°$ is close to the "magic" angle ($\Theta = 54.74°$), where a 1° change in $\Theta$ alters $R$ only by ~7% compared with 75% for the same 1° change in $\Theta$ near 90° or 0°. However, the method used is accurate enough to detect a <1° change in $\Theta$ (Fig. 5).

Thus, the S1-induced change in geometry of Tm in reconstituted thin filament detected by the in vitro fluorescence energy transfer experiments, using the same label (Lehrer and Ishii, 1988), does not appear to involve a change in probe angle.

TABLE 1 **The dichroic ratio, $R = F(\psi = 0°)/F(\psi = 90°)$, and the angle between the probe dipole and fibril axis, $\Theta$, for the actin-bound labeled proteins in myofibrils**

| System | $R$ | $\Theta$ | $n$ |
|---|---|---|---|
| | | degrees | |
| IATR-S1 | 0.68 ± 0.05 | 59.8 ± 0.9 | 15 |
| IATR-S1[ADP] | 1.42 ± 0.04 | 49.9 ± 0.4 | 10 |
| ACS1 ± Tm | 0.60 ± 0.05 | 61.3 ± 1.0 | 52 |
| ACS1[ADP] ± Tm | 0.68 ± 0.05 | 59.8 ± 0.9 | 47 |
| ACTm | 1.21 ± 0.09 | 52.1 ± 1.0 | 93 |
| ACTm + S1 | 1.22 ± 0.11 | 52.0 ± 1.3 | 82 |
| ACTm + S1[ADP] | 1.11 ± 0.06 | 53.3 ± 0.7 | 77 |
| sACTm ± S1 | 1.40 ± 0.10 | 50.1 ± 1.0 | 39 |
| ACTm paracystals | 1.15 ± 0.06 | 52.9 ± 0.7 | 27 |

Errors are the standard deviation of $n$ measurements made.

## DISCUSSION

### Advantages of FDLD

The advantages of FDLD using a high NA objective over the alternate fluorescence polarization technique, which requires a low NA objective, were discussed by Borejdo et al. (1982), who first applied FDLD to oriented muscle systems. These advantages include high sensitivity and

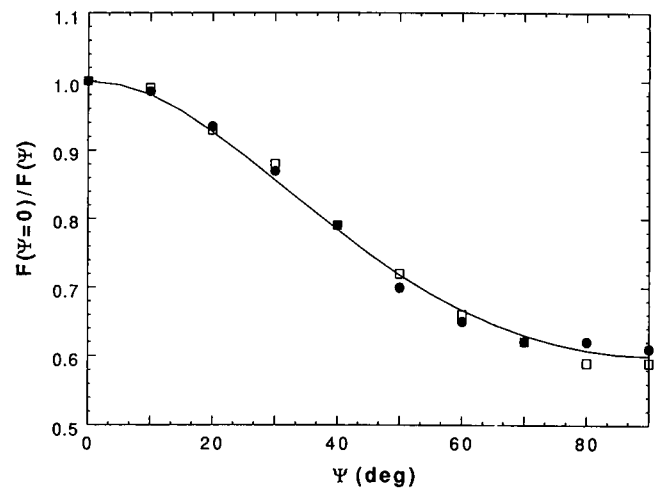


FIGURE 4 The angular dependence of the fluorescence intensity of ACS1 bound to actin in a ghost myofibril. $\psi$ is the angle between the direction of polarization of the excitated light and the myofibril axis. Fluorescence data were obtained for fibrils oriented parallel (●) and perpendicular (□) to the axis of microscope. Solid line represents the best fit of experimental data using Eq. 1 with $\Theta = 61.3°$.

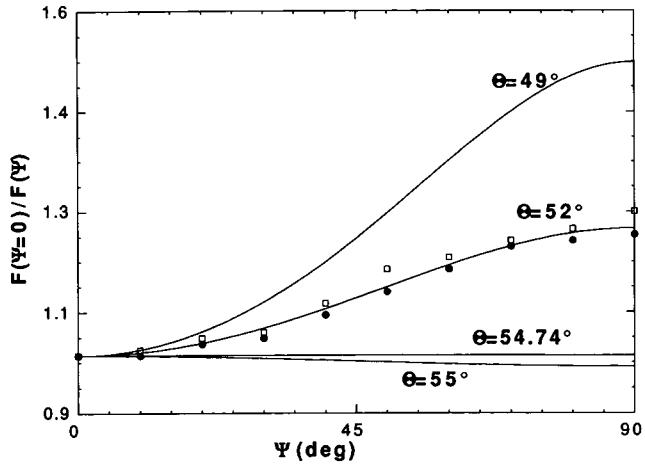


FIGURE 5 The angular dependence of the fluorescence intensity of ACTm bound to actin in a ghost myofibril. $\psi$ is the angle between the direction of polarization of the excitation and the myofibril axis. Fluorescence data were obtained for fibrils oriented parallel (●) or perpendicular (□) to the axis of the microscope. Solid lines are theoretical curves drawn for $\Theta = 49°$, 52°, and 55°, using Eq. 1 to show sensitivity of calculation. Note that for $\Theta = 54.74°$ ("magic" angle) the ratio $F(\psi = 0°)/F(\psi) = 1$ for any $\psi$.

simplicity of analysis, allowing observation of small volumes. For muscle systems, the use of the small diameter fibrils ($\simeq 1$ μm) that are stuck to the coverslip offers a stabilized system from which components can be quickly removed, incorporated again, and visualized; e.g., we observed fluorescence of ACTm or ACS1 bound to the I-bands within seconds after introducing the labeled protein into the microscope cell. The separated fibrils in the field allows for ease in subtracting nonspecific background fluorescence by simply moving the small aperture slightly off the fibril. The larger fibers usually used in polarization measurements cannot be manipulated easily and also cannot be easily visualized during experiments, i.e., it is impossible to observe the highly oriented sarcomeres and the incorporation of other proteins with the use of phase contrast.

## Effects of probe disorder

Dichroism values obtained from FDLD are averages over the whole orientational distribution and the probe angular disorder must be estimated by other methods. Disorder can be dynamic or static. A measure of dynamic disorder can be obtained from the anisotropy ($r$) of ACTm measured under the conditions of the FDLD experiment compared with the immobilized value, $r_0$. For the parent fluorophore, prodan, $r_0 = 0.33$ (Weber and Farris, 1979; Prendergast et al., 1983). From a Perrin plot of ACTm in solution (Lehrer and Ishii, 1988) we obtained $r_0 = 0.32$ at 410 nm after a small correction for the difference in the observed wavelength. At room temperature for ACTm in solution, where $r = 0.26$ (Lehrer and Ishii, 1988), the maximum angle through which the probe rotates during its lifetime is estimated to be $\sim 20°$ (Lakowicz, 1983). It is expected that $r$ may even be greater for ACTm bound to actin in the attached fibrils, and thus the probe is only slightly disordered during its lifetime by dynamic rotation.

A high degree of static disorder is not expected in the fibril system in view of the specific labeling at only one site in the tropomyosin sequence and its specific fluorescence properties indicating a relatively homogeneous environment (Lehrer and Ishii, 1988). Also, a small number of highly oriented sarcomeres are selected for measurement with the aperture. For the paracrystal system, some disorder may be present from flaring of filaments at the ends of the tactoids. An estimate of the disorder of the probe in these systems can be obtained by comparing the dichroic ratio values for the fibrils with those obtained for the paracrystals, with the assumption that the probe polar angle is the same in the paracrystal and in the fibril. This assumption is reasonable because the pitch of the Tm coiled-coil helix in the crystal (135–145 Å) (Phillips et al., 1986) encompasses the value calculated for equivalent interactions with actin in muscle (137 Å) (McLachlan and Stewart, 1975) and is not expected to vary much in different crystal forms. This disorder was estimated with the use of Eq. 5 by the modeling the affect on $R'$ for increasing widths of the Gaussian distribution, $\sigma$, centered around the average $R'$ value (1.18) for the fibril and paracrystal (Fig. 6). By

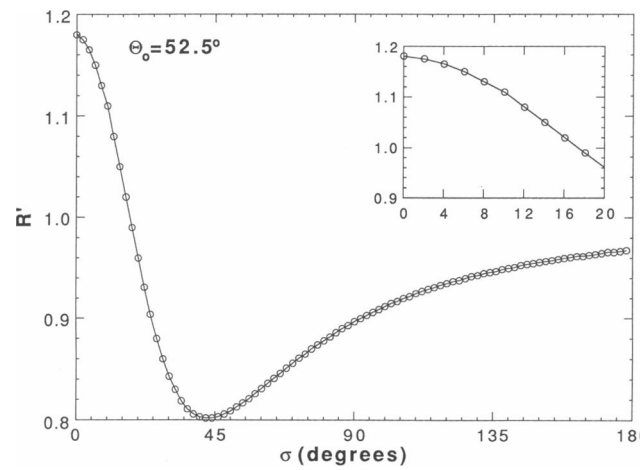


FIGURE 6 Theoretical curve for dependence of $R'$ on width of Gaussian distribution, $\sigma$, for $\Theta_0 = 52.5°$, the average value for ACTm in fibrils and paracrystals. (*Inset*) Expanded view of $R'$ for $0° < \sigma < 20°$. Note that $\sigma < 10°$ corresponds to $\Delta R'/R' < 6\%$.

this method it was found that the measured difference, $\Delta R' \simeq 0.06$, corresponds to $\sigma \simeq 9°$ around the average value of the polar angle, $\Theta_0 = 52.5°$. This distribution width is similar to that estimated for dynamic disorder where the half angle through which the probe rotates is $\simeq 10°$ (see above). A smaller variation in average angle $\Delta\Theta = \pm 1°$ (Table 1) was obtained from the standard deviation of $R$ taken from many measurements ($\pm 0.1$). Thus, it appears that the static and dynamic disorder in these systems is not great.

## Models of S1-induced Tm movement

In the present study we show that the dichroism of ACTm is slightly positive with a polar angle, $\Theta \simeq 52°$, which does not change upon binding S1. It is possible for movement to take place without a change in probe angle as long as the Tm molecular axis remains parallel to the thin filament axis, if there is no S1-induced local distortion of a flexible structure in the region of Cys 190. Although Tm appears somewhat flexible in solution (Flicker et al., 1982; Mabuchi, 1990) and in the crystal where there are few intermolecular contacts (Phillips et al., 1986), when bound to actin it appears to be quite rigid. For example, the thermal pretransition that unfolds ~20% of the helix is inhibited when Tm is bound to actin (Ishii and Lehrer, 1985). Also, because the random binding of 1–2 S1/7 actin in the 1 Tm /7 actin unit is sufficient to completely change the fluorescence properties of various probes at Cys 190 (Ishii and Lehrer, 1985, 1990; Lehrer and Ishii, 1988) it appears to change state as a rigid unit. If Tm were flexible, it would be expected that the fluorescence would rather gradually change as more S1 is bound to actin.

There are two general models involving large movements of Tm on actin that have been proposed for the changing Tm–actin interaction associated with regulation. The model of McLachlan and Stewart (1976) extended by Parry (1976) suggests, on the basis of amino acid sequence repeats, that there are two sets of seven actin-binding sites on Tm that could alternatively be used by a 90° rotation of Tm on the actin filament. The model of Phillips et al. (1986) proposed on the basis of the site geometry of the sequence repeat, suggests that there is only one set of seven actin-binding sites. Increases in the strength of interaction of Tm with actin associated with $Ca^{2+}$ binding to troponin and further with S1 binding is suggested to cause the Tm molecule to shift closer to the actin surface, with a parallel translation of Tm without much rotation. Our data appear consistent with either model because in both models the Tm axis remains parallel to the actin axis.

In conclusion, the binding of myosin heads to Tm–actin in myofibrils does not change the polar dipole angle of a fluorescence probe specifically attached to Tm relative to the actin axis. It appears that the fluorescence energy transfer change, detected earlier in vitro using the same label on Tm, and the postulated movement of Tm associated with activation of the thin filament, involves a movement that maintains the relative orientation of the Tm and actin helices and does not distort the Tm structure near the probe.

Some preliminary experiments were done in the laboratory of Dr. J. Borejdo. We thank him and Dr. T. Burghardt for helpful comments, Drs. C. Coppin and Z. Grabarek for help in computer programming, Dr. Y. Ishii for help with some of the solution experiments, and Dr. S. Hvidt for the sample of frog ααTm.

This work was done during the tenure of a research fellowship from the American Heart Association, Massachusetts Affiliate, Inc. (to Danuta Szczesna). Supported also by grants from NSF (DMB 8817581) and NIH (HL-22461) (to Sherwin Lehrer).

*Received for publication 7 August 1991 and in final form 29 October 1991.*

## REFERENCES

Ajtai, K., and T. P. Burghardt. 1987. Probe studies of the MgADP state of muscle cross-bridges: microscopic and wavelength-dependent fluorescence polarization from 1,5-IAEDANS–labeled myosin subfragment 1 decorating muscle fibers. *Biochemistry.* 26:4517–4523.

Borejdo, J., S. Putnam, and M. F. Morales. 1979. Fluctuations in polarized fluorescence: evidence that muscle cross bridges rotate repetitively during contraction. *Proc. Natl. Acad. Sci. USA.* 76:6346–6350.

Borejdo, J., O. Assulin, T. Ando, and S. Putnam. 1982. Cross-bridge orientation in skeletal muscle measured by linear dichroism of an extrinsic chromophore. *J. Mol. Biol.* 158:391–414.

Bremel, R. D., and A. Weber. 1972. Cooperation within actin filament in vertebrate skeletal muscle. *Nature (Lond.).* 238:97–101.

Burghardt, T. P., T. Ando, and J. Borejdo. 1983. Evidence for cross-bridge order in contraction of glycerinated skeletal muscle. *Proc. Natl. Acad. Sci. USA.* 80:7515–7519.

Burghardt, T. P., and N. L. Thompson. 1984. Effect of planar dielectric interfaces on fluorescence emission and detection. *Biophys. J.* 46:729–737.

Caspar, D. L. D., C. Cohen, and W. Longley. 1969. Tropomyosin: crystal structure, polymorphism and molecular interactions. *J. Mol. Biol.* 41:87–107.

Englander, S. W., D. B. Calhoun, and J. J. Englander. 1987. Biochemistry without oxygen. *Anal. Biochem.* 161:300–306.

Flicker, P. F., G. N. Phillips, Jr., and C. Cohen. 1982. Troponin and its interactions with tropomyosin. *J. Mol. Biol.* 162:495–501.

Goldman, Y. E., M. G. Hibberd, and D. R. Trentham. 1984. Relaxation of rabbit psoas muscle fibres from rigor by photochemical generation of adenosine-5′-triphosphate. *J. Physiol. (Lond.).* 354:577–604.

Gordon, A. M., E. B. Ridgway, L. D. Yates, and T. Allen. 1988. Muscle cross-bridge attachment: effects on calcium binding and calcium activation. *Adv. Exp. Med. Biol.* 226:89–99.

Guth, K., and J. D. Potter. 1987. Effect of rigor and cycling cross-bridges on the structure of troponin C and on the $Ca^{2+}$ affinity of the $Ca^{2+}$-specific regulatory sites in skinned rabbit psoas fibers. *J. Biol. Chem.* 262:13627–13635.

Haselgrove, J. C. 1972. X-ray evidence for a conformational change in actin-containing filaments of vertebrate striated muscle. *Cold Spring Harbor Symp. Quant. Biol.* 37:341–352.

Huxley, H. E. 1972. Structural changes in the actin- and myosin-containing filaments during contraction. *Cold Spring Harbor Symp. Quant. Biol.* 37:361–376.

Hvidt, S. 1986. Differences in thermal stability of frog and rabbit αα- and αβ-tropomyosins determined by optical rotatory dispersion. *Biophys. Chem.* 24:211–215.

Ishii, Y., and S. S. Lehrer. 1985. Fluorescence studies of the conformation of pyrene-labeled tropomyosin: effects of F-actin and myosin subfragment 1. *Biochemistry.* 24:6631–6638.

Ishii, Y., and S. S. Lehrer. 1987. Fluorescence probe studies of the state of tropomyosin in reconstituted muscle thin filaments. *Biochemistry.* 26:4922–4925.

Ishii, Y., and S. S. Lehrer. 1990. Excimer fluorescence of pyrenyliodoacetamide-labeled tropomyosin: a probe of the state of tropomyosin in reconstituted muscle thin filaments. *Biochemistry.* 29:1160–1166.

Ishii, Y., and S. S. Lehrer. 1991. Two-site attachment of troponin to pyrene-labeled tropomyosin. *J. Biol. Chem.* 266:6894–6903.

Lakowicz, J. R. 1983. Principles of Fluorescence Spectroscopy. Plenum Press, New York. 134–139.

Lehrer, S. S., and Y. Ishii. 1988. Fluorescence properties of acrylodan-labeled tropomyosin and tropomyosin-actin: evidence for myosin subfragment 1 induced changes in geometry between tropomyosin and actin. *Biochemistry.* 27:5899–5906.

Lehrer, S. S., and E. P. Morris. 1982. Dual effects of tropomyosin and troponin-tropomyosin on actomyosin subfragment 1 ATPase. *J. Biol. Chem.* 257:8073–8080.

Mabuchi, K. 1990. Melting of myosin and tropomyosin: electron microscopic observations. *J. Struct. Biol.* 103:249–256.

McLachlan, A. D., and M. Stewart. 1975. Tropomyosin coiled-coil interactions: evidence for an unstaggered structure. *J. Mol. Biol.* 98:293–304.

McLachlan, A. D., and M. Stewart. 1976. The 14-fold periodicity in α-tropomyosin and the interaction with actin. *J. Mol. Biol.* 103:271–298.

Miki, M. 1990. Resonance energy transfer between points in a reconstituted skeletal muscle thin filament. *Eur. J. Biochem.* 187:155–162.

Millar, N. C., and E. Homsher. 1990. The effect of phosphate and calcium on force generation in glycerinated rabbit skeletal muscle fibers. *J. Biol. Chem.* 265:20234–20240.

Nagashima, H., and S. Asakura. 1982. Studies on co-operative properties of tropomyosin-actin and tropomyosin-troponin-actin complexes by the use of *N*-ethylmaleimide-treated and untreated species of myosin subfragment 1. *J. Mol. Biol.* 155:409–428.

Okamoto, Y., and T. Sekine. 1985. A streamlined method of subfragment one preparation. *J. Biochem. (Tokyo).* 98:1143–1145.

Parry, D. A. D. 1976. Movement of tropomyosin during regulation of vertebrate skeletal muscle: a simple physical model. *Biochem. Biophys. Res. Commun.* 68:323–328.

Parry, D. A. D., and J. M. Squire. 1973. Structural role of tropomyosin in muscle regulation: analysis of the x-ray diffraction patterns from relaxed and contracting muscles. *J. Mol. Biol.* 75:33–55.

Phillips, G. N., Jr., J. P. Fillers, and C. Cohen. 1986. Tropomyosin crystal structure and muscle regulation. *J. Mol. Biol.* 192:111–131.

Prendergast, F. G., M. Meyer, G. L. Carlson, S. Iida, and J. D. Potter. 1983. Synthesis, spectral properties, and use of 6-acryloyl-2-dimethylaminonaphthalene (acrylodan). *J. Biol. Chem.* 258:7541–7544.

Szczesna, D., Y. S. Borovikov, I. Kakol, and A. Sobieszek. 1989. Interaction of tropomyosin with F-actin-heavy meromyosin complex. *Biol. Chem. Hoppe-Seyler.* 370:399–407.

Tao, T., M. Lamkin, and S. S. Lehrer. 1983. Excitation energy transfer studies of the proximity between tropomyosin and actin in reconstituted skeletal muscle thin filaments. *Biochemistry.* 22:3059–3066.

Weber, G., and F. J. Farris. 1979. Synthesis and spectral properties of a hydrophobic fluorescent probe: 6-propionyl-2-(dimethylamino)naphthalene. *Biochemistry.* 18:3075–3078.

Weeds, A. G., and B. Pope. 1977. Studies on the chymotryptic digestion of myosin. Effects of divalent cations on proteolytic susceptibility. *J. Mol. Biol.* 111:129–157.

Williams, D. L., Jr., L. E. Greene, and E. Eisenberg. 1988. Cooperative turning on of myosin subfragment 1 adenosinetriphosphatase activity by the toponin-tropomyosin-actin complex. *Biochemistry.* 27:6987–6993.

Yagi, N. 1988. An x-ray diffraction study of α-tropomyosin magnesium tactoid. *J. Muscle Res. Cell Motil.* 9:393–402.

Yanagida, T., and F. Oosawa. 1978. Polarized fluorescence from ε-ADP incorporated into F-actin in a myosin-free single fiber: conformation of F-actin and changes induced in it by heavy meromyosin. *J. Mol. Biol.* 126:507–524.